Diagnosis and optimisation of continuous casting practices through numerical modelling

P. N. Jalali, P. E. R. Lopez, C. Nilsson, P. Hietanen, P. Jönsson

An advanced numerical model has been used to diagnose casting practices for a peritectic grade in a Scandinavian steel producer. The model solves the Navier-Stokes equations by use of an interface tracking technique known as the Volume of Fluid (VOF). Furthermore, the model considers heat transfer, solidification and uses Discrete Phase Model to simulate a multiple phase system of steel, slag and argon. As a result, it is possible to predict the metal flow and slag infiltration as well as their influence on the heat flux and solidification under the effect of gas injection and for transient conditions. Recent improvements to the model include a separation between mould powder and slag film and the consideration of the effect of crystallization on the interfacial resistance for a peritectic mould powder. The casting parameters analysed consist of the casting speed interlocked with oscillation settings, Submerged Entry Nozzle (SEN) immersion depths and argon injection flow rates. These practices were optimised by performing parametric studies to evaluate the shell growth, lubrication depth, cooling channel heat flux, etc. The application of the model allows for a prediction of trends and the results provide opportunities for further improvement in the form of guidelines for the process and enhanced operational windows. The model has been tested under industrial conditions and the results indicate the improvements of the surface quality and process stability can be obtained.

KEYWORDS: CONTINUOUS CASTING - NUMERICAL MODELLING - MOULD OSCILLATION - IMMERSION DEPTH - ARGON INJECTION - SHELL GROWTH

INTRODUCTION

Conventional continuous casting is one of the most cost effective production routes for producing semifinished materials from molten steel. This cost–effectiveness is largely dependent on both quantity and quality of the final products. Therefore, it is essential to control the inter-reliant physical phenomena occurring simultaneously inside the mould such as fluid flow, heat transfer and solidification to provide a smooth and stable casting process. This subsequently decreases the probability of defects (i.e. deep oscillation marks, transverse and longitudinal cracks, etc.) and increases the overall yield in the form of decreased need for surface treatments and a decreased amount of scrapped materials [1, 2].

Pooria Nazem Jalali, Pavel E. Ramirez Lopez
Swerea MEFOS AB, Aronstorpsvägen 1, SE 97 437 Luleå, SWEDEN
Pooria.jalali@swerea.se

Pooria Nazem Jalali, Pär Jönsson
Materials Science and Engineering Department, KTH University, Brinellvägen 23, Stockholm, SWEDEN

Paper presented at the International Conference STEELSIM, Bardolino Italy, 23-25 September 2015, organized by AIM

Application of multifunctional advanced mould powders in combination with more sophisticated casting machines have immensely improved the internal and surface quality of cast products. However, the introduction of newly developed materials and casting of crack sensitive steel grades under more severe casting conditions such as higher casting speeds are unfamiliar territories for casting floor engineers/operators. Thus, this demands further investigations of possibilities to improve the process optimization. For instance, peritectic steel grades are particularly prone to longitudinal cracks and an uneven shell growth due to inappropriate cooling rates. The underlying cause for castability problems in peritectic steels is the δ-Fe to austenite transformation, which is known to lead to: i) a significant variation in the thermal shrinkage coefficient due to the change in the atomic structure from a BCC phase to a FCC phase [3] and ii) a vast change in mechanical strength of the meniscus shell which produces a strong shell at a high ferrite potential (0.85-1.05) where overcomes the ferrostatic pressure and shrinks away from the mould if the local cooling intensity is adequately high [4]. The resultant shrinkage leads to an uneven shell growth and in the worst-case scenario to longitudinal cracks. Therefore, it is absolutely necessary to regulate the cooling rate of the newly formed shell in order to obtain a defect free and smooth shell growth.

Normally, casting setups for newly developed materials are chosen by finding the closest composition already in production and by tuning the settings by trial and error tests. As expected, this procedure is rather expensive and only allows for the introduction of new materials in an "incremental" way. Furthermore, the number of variables involved in the casting process is very large (e.g. casting speed, SEN immersion depth, argon flow rate, mould oscillation, etc.) which makes it difficult to assess the effects that changes in one parameter would have on the rest of the parameters and vice-versa. Therefore, advanced multiphase numerical models capable of coupling different physical phenomena are required to investigate the complex phenomena which occur in the caster in order to reduce the gap between plant trials and a smooth mass production as well as to increase the casting efficiency by reducing the number of defects and costs due to the need for trial and error tests.

NUMERICAL MODEL

Methodology and computational domain

The present work deals with the industrial application of the prior models developed by the authors [1, 5-9] which investigate the performance of a conventional slab caster. The model solves the Navier-Stokes equations by use of an interface tracking technique known as the Volume of Fluid (VOF) technique [10] to calculate phase fractions. Furthermore, the Continuum Surface Force (CSF) method [11] is used to determine the effect of the surface tension at the meniscus. In this approach, a volume average value of the field variables and properties are calculated and are assigned to computational cells based on the computed volume fraction of each phase. Therefore, the calculated variables or properties in the computational cells represents either one pure phase or a mixture of two phases [6]. For instance, the mixture density (ρ_{mix}) and viscosity (μ_{mix}) are calculated as follows; see Equations 1 and 2:

$$\rho_{mix} = \alpha_x \rho_x + (1-\alpha_x)\rho_y \tag{1}$$

$$\mu_{mix} = \alpha_x \mu_x + (1-\alpha_x)\mu_y \tag{2}$$

where, (α) specifies the phase fraction and the subscripts (x) and (y) indicate any two of the phases in the cell [12]. In the VOF method, a single set of equations is solved for momentum, which comprises the mixture density and viscosity of the phases; see Equation 3.

$$\frac{\partial}{\partial t}(\rho_{mix}\vec{v}) + \nabla.(\rho_{mix}\vec{v}\vec{v}) = -\nabla P + \nabla.\left[\mu_{mix}\left(\nabla\vec{v} + \nabla\langle -\frac{2}{3}\nabla.\vec{vI}\rangle\right)\right] + \rho_{mix}\vec{g} - S_s + S_\gamma \quad (3) \tag{3}$$

The terms (∇p) and ($\vec{g}$) denote the pressure difference and gravitational force vector. The last two terms (S_s) and (S_γ) represent momentum sinks created by solidification and interfacial tension phenomena, respectively[6].

The fluid flow model is also coupled with heat transfer, solidification and Discrete Phase Model (DPM). The solidification model for the steel phase is based on an enthalpy porosity technique [12], where the mushy zone region is regarded as a porous medium. The amount of porosity is calculated based on liquid fraction f_l where regions composed of 100% solid are considered to have zero porosity [12]; see Equation 4.

$$f_l = \frac{T - T_{solidus}}{T_{liquidus} - T_{solidus}} \tag{4}$$

Effectively, this approach creates a solidification front at $T_{liquidus}$, a mushy zone between ($T_{liquidus}$-$T_{solidus}$), and a solid shell below $T_{solidus}$. Finally, the calculated shell thickness is modified by the Zero Strength Temperature (ZST) which is equivalent to a 0.7 solid fraction and is assumed to ensure an adequate strength to be pulled down at the casting speed [13].

Argon gas is normally injected during the process in order to reduce the clogging occurrence as well as to enhance the liquid steel cleanliness. The current model employs an Euler-Lagrangian approach [14-18], which treats the steel phase as a continuum by solving the Navier-Stokes equations. Furthermore, the discrete phase representing argon bubbles is solved by tracking the particles through the calculated flow field. In addition, a modified drag force function based on the Eotvos number [19] is used instead of using the FLUENT DPM standard spherical and non-spherical drag functions. The modified drag force improves the bubbles behavior and shows a better agreement with experimental results [7]. In this study, the bubbles diameter and frequency are calculated based on the results by Iguchi et al. [20].

The recent industrial application of the coupled VOF-DPM method should be credited to Cloete et al. [19, 21], who implemented the technique for ladle metallurgy. The combined VOF-DPM method in the current work is based on such prior work, but has been adapted to continuous casting operations. This is done by making an addition of mould powder to the steel bath, where it is heated up to create a sintered layer as well as a liquid slag pool. The corresponding physical properties of the solid, liquid and powdered states are defined as a function of the temperature and position and they have been implemented through the use of a User Defined Function. The fundamentals behind the employed numerical models can be found in the ANSYS-FLUENT theory guide [12].

Figure 1 is a schematic illustration of a casting mould showing the solidifying shell, slag layers and total horizontal thermal resistance R_{total} for both fully and interrupted lubricated regions. The fully and interrupted lubricated regions are distinct by the absence of a liquid slag layer (R_{liquid}) and the formation of an air gap (Rair gap) in the interrupted lubricated area; see Figure 1.

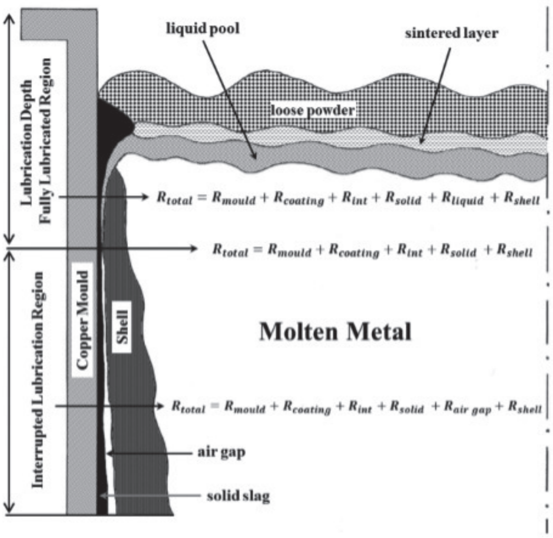

Fig. 1 - A schematic illustration of a continuous casting mould [8]

This could be explained by a shell contraction during solidification and an inappropriate mould taper. In the current model, the powder break temperature T_{br} is used to differentiate interrupted and fully lubricated regions from each other. This is due to that the shell contraction is not included in the calculations. Also the interfacial thermal resistance (R_{int}) is linked to the crystalline slag layer and it is obtained from Cho et al. [22] work. In general, it increases with an increased thickness of the slag film as well as with the degree of crystallinity.

Figure 2 shows the boundary conditions applied to the 2D computational domain. The computational domain is composed of half of the caster central plane, including the SEN, copper mould and cooling water channels as well as 1m of the strand length after the mould exit.

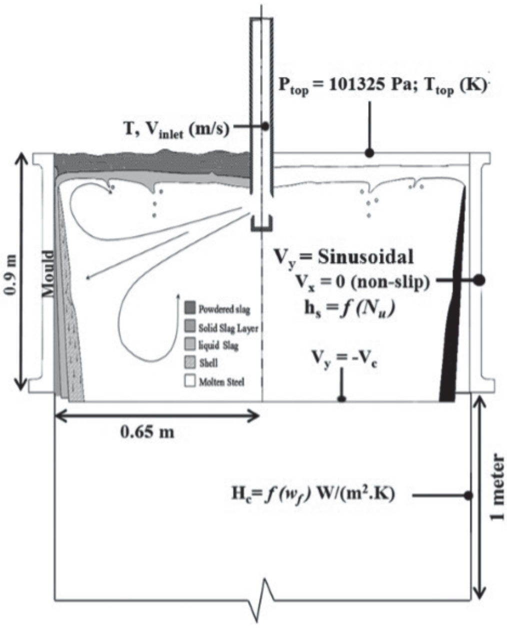

Fig. 2 - A schematic illustration of the involved phases, boundary conditions and domain geometry [7]

The treatment of heat extraction is considered through the use of two constant convection heat transfer coefficients based on the Nusselt number [23] and water flow rates [24] measured on-plant for primary and secondary cooling regions, respectively. Also, the mould oscillation parameters (e.g. stroke and frequency) are linked to the casting speed and are implemented through a User Defined Function. Equation 5 shows the mould velocity function for a sinusoidal mode [25].

$$V_m = 2\pi af\cos(2\pi ft) \tag{5}$$

where, f, a and t represent oscillation frequency, amplitude and time, respectively. Full details of the solution methods, computational mesh and boundary conditions have been published elsewhere [1, 5, 6, 9].

Design of Experiment and Simulation Matrix

A matrix of simulations based on Design of Experiment (DOE) software has been defined for a peritectic steel grade cast using a constant pouring temperature. The DOE analysis exploits a second order BOX Behnken model [26] and includes 13 different casting setups; see Table 1.

This study explores the interrelation between the casting speed (m/min), SEN immersion depth (mm) and argon injection rate (lit/min) to investigate the effect of these parameters on the mould powder performance and process stability.

Specifically, this study is aimed at:

- Predicting the transient slag infiltration and shell lubrication
- Describing the transient shell formation
- Finding the optimal casting conditions to minimize the formation of defects

Tab. 1 - Designated simulation matrix used in the parametric study

Exp. no	Casting Speed	Immersion Depth	Ar Flow
1	Low	Shallow	Medium
2	Low	Medium	Low
3	Low	Medium	High
4	Low	Deep	Medium
5	Medium	Shallow	Low
6	Medium	Shallow	High
7	Medium	Medium	Medium
8	Medium	Deep	Low
9	Medium	Deep	High
10	High	Shallow	Medium
11	High	Medium	Low
12	High	Medium	High
13	High	Deep	Medium

RESULTS AND DISCUSSION

There are various techniques and methods to obtain data from ANSYS-FLUENT. Providing results in the form of plots, contours and also recording data from monitoring points are the most common approaches. In the current model, a series of tracking points at different positions in the domain are defined in order to track various features of interest such as the shell thickness, cooling channels heat flux, slag film thickness, etc. These points are mainly located at 100 and 50 mm below the meniscus to analyze the behavior of newly formed meniscus shell and at the mould exit. The following are few examples of obtained results from simulations where all the acquired results have been normalized.

Regression Equations

A full statistical analysis was carried out based on the acquired data from simulations matrix. This led to the derivations of governing regression equations. These do not only describe the relationships between the casting settings and the process parameters, but also explain that to what extend these parameters are affecting the casting stability. As an example of regression results, Equation 6 shows the effect of the casting speed (V), SEN immersion depth (D) and argon injection rate (F) on the lubrication index (LI).

$$LI = b_0 + b_1.D + b_2.V + b_3.F + b_4.D^2 + b_5.V^2 + b_6.F^2 + b_7.D.V + b_8.D.F + b_9.V.F \quad (6)$$

where, b0-b9 are the regression coefficients. Lubrication index describes how deep liquid slag infiltrates into the mould-shell channel and can be used as a measure for the mould powder lubrication efficiency.

Variable Immersion Depth

The effect of a variable immersion depth, which is a typical practice in the casting floor, on the production has been studied through analyse of shallow, medium and deep positions of the SEN. Figures 3 and 4 illustrate the influence of shallow and deep SEN immersion depths on the lubrication index, slag film thickness at a position 100 mm below the meniscus, the channels heat flux and the shell thickness at the mould exit under an analogous casting speed (low) and argon flow rate (medium).

The results show that the SEN immersion depth has an enormous effect on the slag infiltration; see Figure 3. The model predictions show a ~22% larger and a ~6% thicker LI and slag thickness for a shallow position compared to a deep immersion depth, respectively. This effect could be explained by a colder meniscus for the deep immersion depth due to a weaker upper roll. Thus, has a negative effect on slag infiltration into the mould-shell channel.

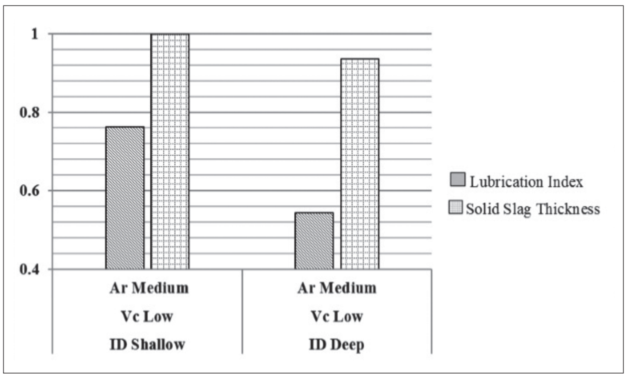

Fig. 3 - Variation of the lubrication index and solid slag film thickness at different SEN immersion depths

The model is also able to capture the effect of the immersion depth on the amount of heat extraction through the cooling channels. Basically, the amount of slag infiltration into the mould-shell channel defines how much heat is absorbed by the cooling water. The Predicted channels heat flux and resultant shell thickness at the mould exit is illustrated in Figure 4 . The deep position provides a ~5% higher channel heat flux, which consequently leads to formation of a ~4% thicker shell compared to the shallow position. This behaviour explains the uneven shell growth and thickness variations in the casting direction under similar casting conditions, which will have a negative impact on the production quality.

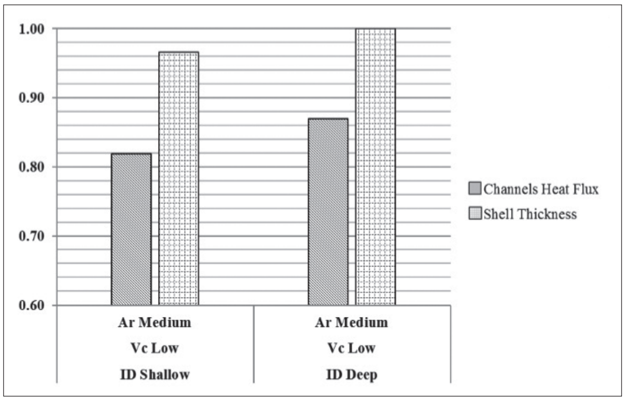

Fig. 4 - Variation of the shell thickness and channels heat flux at different SEN immersion depths

The simulation results also show that the effect of a variable immersion depth is larger at higher casting speeds than at lower casting speeds. A 50% increased of the casting speed results in almost a 7% difference in the shell thickness for a similar SEN displacement and argon injection rate; see Figure 5. Based on the acquired results, a shorter SEN displacement is recommended in order to minimize the irregular shell formation by producing a more uniform heat transfer within the mould.

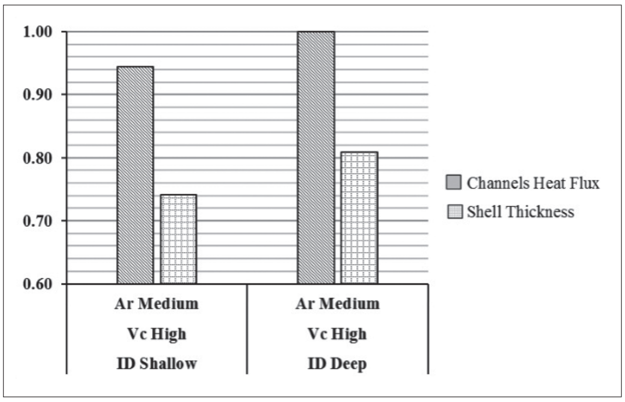

Fig. 5 - The effect of the SEN immersion depth on the heat flux and shell thickness at a high casting speed

Casting Speed and Argon Flow Rate Effects

The casting speed is one parameter which plays an important role on the process stability and final product quality. For instance, breakouts and slag entrapment due to surface waves and a turbulent flow close to the steel-slag interface are deeply affected by the SEN design [27] and casting speed. Figure 6 shows the influence of the casting speed on the shell lubrication at different immersion depths.

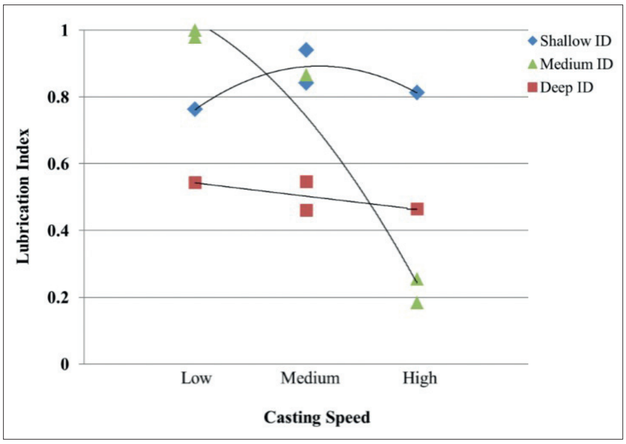

Fig. 6 - Effect of the casting speed and SEN immersion depth on the shell lubrication

The results show that although a medium immersion depth provides a high lubrication at low and medium casting speeds, the solidifying shell suffers from a lack of lubrication at high casting speeds. Furthermore, a deep SEN position produces a small but a uniform lubrication to the shell. Based on the simulation results, it is seen that a shallow immersion depth forms a stable slag layer, which creates a maximum infiltration for a wide range of casting speeds. Therefore, it is recommended to avoid a combination of a high casting speed and a medium immersion depth, which is detrimental to lubrication efficiency and also to minimize the residence time at deep immersion depth due to low slag infiltration depth.

The effects of the casting speed and argon flow rate on the channels heat flux, shell and solid slag thickness are shown in Figure 7 at a shallow immersion depth. The results indicate a minor effect of the argon flow rate on the predicted parameters whereas as it was expected, the shell growth and the slag thickness decrease when the casting speed is increased. In contrast, the channel heat flux increases when the casting speed is increased from a low to a high speed. For example, a high casting speed produces almost a 23% thinner shell compared to a low casting speed; see Figure 7.

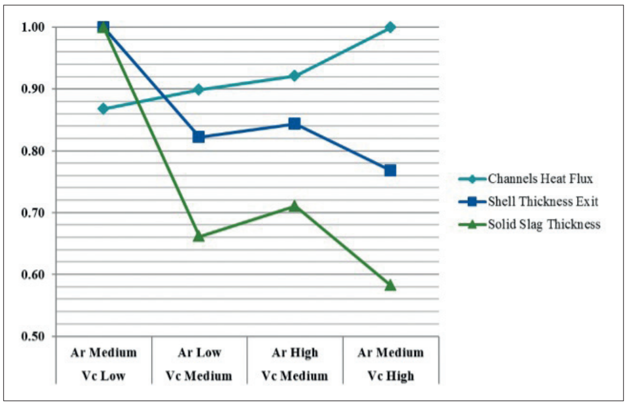

Fig. 7 - Effect of the casting speed and argon flow rate on the casting parameters at shallow ID

Figures 8 (a-c) are 3D illustrations of the influence of the casting speed and argon injection on the shell growth at different immersion depths of the SEN.

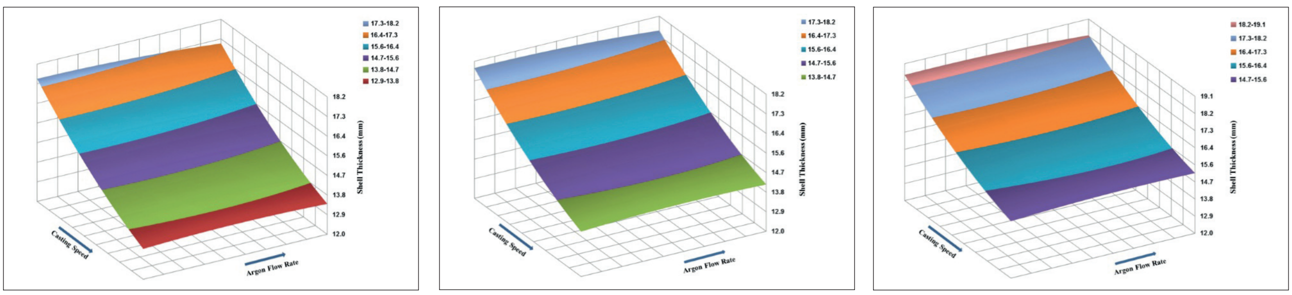

(a) (b) (c)

Fig. 8 - Effect of the casting speed and argon flow rate on the shell growth at a) a shallow, b) a medium, and c) a deep immersion depth of the SEN

As was shown earlier, the acquired results emphasise major effects of the casting speed and immersion depth on the solidification, whereas the argon flow rate produces a minor effect on the shell growth. The argon influence is more perceptible at low casting speeds. For instance, a combination of a low casting speed and a high argon flow rate has a negative impact on the shell growth rate; see Figure 8(a-c). This could be explained by larger bubbles compared to low argon flow rates, which create a distinctive behaviour in the bubble departure within the mould.

Based on the results and previous experience [7], the low argon flow rate have a tendency to provide a more uniform distribution of bubbles, which are transported deeper into the mould by the discharging jet. In contrast, high argon flow rates leads to the formation of larger bubbles that tend to rise closer to the SEN, due to enhanced buoyancy and drag forces. This subsequently weakens the discharging jet and disturbs the heat transportation within the mould. These disturbances can also be seen in Figure 9, which illustrates the effect of the casting speed and argon flow rate on the channels heat flux at shallow immersion depths. Specifically, it is seen that a high casting speed leads to almost a 26% higher heat flux compared to a low casting speed.

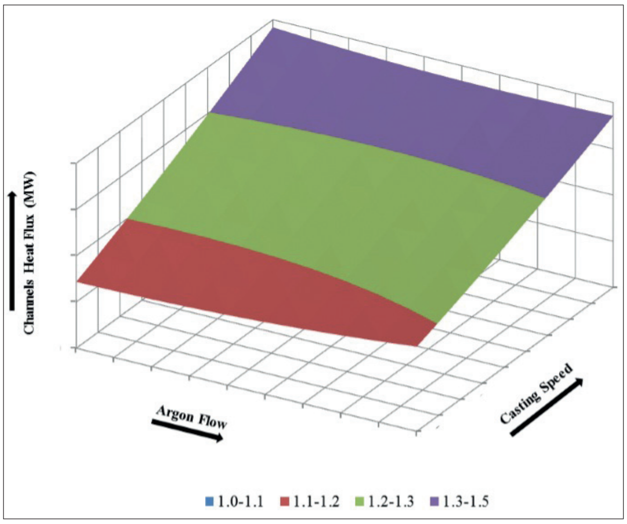

Fig. 9 - Effect of the casting speed and argon flow rate on the channels heat flux at a shallow immersion depth

CONCLUSIONS

A 2D numerical model including the interactions between the mould powder and steel grade was developed. The model was used to simulate a series of casting setups for a peritectic steel grade under transient conditions. The results show that the model is able to capture the effect of different casting parameters on the process stability and has the potential to be applied as a benchmark to diagnose and analyse different continuous casting practices. Based on the performed parametric study and a DOE analysis the following recommendations were proposed to the casting floor engineers in order to enhance casting stability and production yield:

- Reduce the SEN displacement in order to create a uniform heat distribution within the mould, which is extremely beneficial to prevent an irregular shell growth and to increase the product quality.
- Avoid high argon injection flow rates, due to their negative effect on the flow pattern and consequently heat distribution within the mould.
- Minimize the time that the SEN spends at the deep position since it reduces the slag infiltration due to cold meniscus which is detrimental to the product surface quality.
- Avoid high casting speeds in combination with large SEN displacements which, creates a thin solidifying shell with a large variation in thickness.

These changes have been tested at the caster with considerable reductions in the number of defects such as longitudinal cracks. This has resulted in a decreased amount of scarfing. Due to these improvements, a new immersion depth strategy with tighter displacements was implemented at the caster.

Acknowledgements

The authors would like to thank casting floor engineers and operators at SSAB Luleå for fruitful discussions and support during the project. The research leading to these results has received funding from the European Union's Research Programme of the Research Fund for Coal and Steel (RFCS) under grant agreement n° [RFSR-CT-2011-00005].

REFERENCES

[1] Ramirez-Lopez, P.E., et al., A new approach for modelling slag infiltration and solidification in a continuous casting mould. ISIJ International, 2010. 50(12): p. 1797-1804.

[2] Thomas, B.G. On-line detection of quality problems in continuous casting of steel. in Proceedings of Modeling, Control and Optimization in Ferrous and Nonferrous Industry Symposium. 2003.

[3] Mills, K.C., et al., Performance and properties of mould fluxes. Ironmaking & steelmaking, 2005. 32(1): p. 26.

[4] Wolf, M. Strand Surface Quality and the Peritectic Reaction - A Look into the Basics. in ATEELMAKING CONFERENCE PROCEEDINGS. 1998.

[5] Ramirez Lopez, P.E., P.D. Lee, and K.C. Mills, Explicit modelling of Slag Infiltration and Shell Formation during Mould Oscillation in Continuous Casting. ISIJ International, 2010. 50(3): p. 425-434.

[6] Ramirez Lopez, P.E., Modelling Shell and Oscillation Mark Formation during Continuous Casting via Explicit Incorporation of Slag Infiltration, in Materials2010, Imperial College London: London. p. 170.

[7] Ramirez Lopez, P.E., et al., Recent developments of a numerical model for continuous casting of steel: Model theory, setup and comparison to physical modelling with liquid metal. ISIJ International, 2014. 54(2): p. 342-350.

[8] Nazem Jalali, P., et al., Analysing The Performance Of Mould Powders For Niche Steels Through Advanced Numerical Modelling, in 8th European Continuous Casting Conference2014, ASMET: Graz, Austria.

[9] Nazem Jalali, P., Analysis of Different Continuous Casting Practices Through Numerical Modelling, in Department of Materials Science and Engineering2013, Royal Institute of Technology: Stockholm. p. 25.

[10] Liow, J.L., M. Rudman, and P. Liovic, A volume of fluid (VOF) method for the simulation of metallurgical flows.

ISIJ international, 2001. 41(3): p. 225-233.
[11] Brackbill, J.U., D.B. Kothe, and C. Zemach, A continuum method for modeling surface tension. Journal of Computational Physics, 1992. 100(2): p. 335-54.
[12] ANSYS-FLUENT, ANSYS Fluent Theory Guide, 2013, ANSYS Inc.
[13] Mazumdar, S. and S.K. Ray, Solidification control in continuous casting of steel. Sadhana, 2001. 26(1-2): p. 179-198.
[14] Cross, M., et al., Computational modelling of bubbles, droplets and particles in metals reduction and refining. Applied mathematical modelling, 2006. 30(11): p. 1445.
[15] Tabib, M.V., S.A. Roy, and J.B. Joshi, CFD simulation of bubble column—An analysis of interphase forces and turbulence models. Chemical Engineering Journal, 2008. 139(3): p. 589-614.
[16] Díaz, M.E., et al., Numerical simulation of the gas–liquid flow in a laboratory scale bubble column: Influence of bubble size distribution and non-drag forces. Chemical Engineering Journal, 2008. 139(2): p. 363-379.
[17] Zhang, D., N.G. Deen, and J.A.M. Kuipers, Numerical simulation of the dynamic flow behavior in a bubble column: A study of closures for turbulence and interface forces. Chemical Engineering Science, 2006. 61(23): p. 7593-7608.
[18] Jakobsen, H.H., Phase distribution phenomena in two-phase bubble column reactors. Chemical engineering science, 2001. 56(3): p. 1049-1056.
[19] Olsen, J.E. and S.W.P. Cloete, COUPLED DPM AND VOF MODEL FOR ANALYSES OF GAS STIRRED LADLES AT HIGHER GAS RATES, in Seventh International Conference on CFD in the Minerals and Process Industries2009, CSIRO: Melbourne, Australia
[20] Iguchi, M., et al., X-ray fluoroscopic observation of bubble characteristics in a molten iron bath. Isij International, 1995. 35(11): p. 1354-1361.
[21] Cloete, S.W.P., J.J. Eksteen, and S.M. Bradshaw, A mathematical modelling study of fluid flow and mixing in full-scale gas-stirred ladles. Progress in Computational Fluid Dynamics, 2009. 9(6-7): p. 345-356.
[22] Cho, J., et al., Thermal resistance at the interface between mold flux film and mold for continuous casting of steels. ISIJ international, 1998. 38(5): p. 440.
[23] Gonzalez, M., et al., Modeling of the Solidification Process in a Continuous Casting Installation for Steel Slabs. Metallurgical and materials transactions. B, Process metallurgy and materials processing science, 2003. 34B(4): p. 455.
[24] Thomas, B.G., J.M. Wells, and J. Sengupta, The use of water cooling during the continuous casting of steel and aluminum alloys. Metallurgical and materials transactions. A, Physical metallurgy and materials science, 2005. 36A(1): p. 187-204.
[25] Elfsberg, J., Oscillation Mark Formation in Continuous Casting Processes, in Materials2003, Royal Institute of Technology: Stockholm, Sweden. p. 56.
[26] Steppan, D.D., J. Werner, and R.P. Yeater, Essential Regression and Experimental Design for Chemists and Engineers, 1998.
[27] F. M. Najjar, B. G. Thomas, and D.E. Hershey, Numerical study of steady turbulent flow through bifurcated nozzles in continuous casting Metallurgical and Materials Transactions B, 1995. 26(4): p. 749-765.